Dawson, and G. C. Neilson, Nucl. Phys. A134, 141 (1969).
[6]N. A. Brown, Ph. D. thesis, Rice University, 1963 (unpublished); N. A. Brown and C. M. Class, Bull. Am. Phys. Soc. 8, 127 (1963).
[7]A. Marinov, C. Drory, E. Navon, J. Burde, and G. Engler, Phys. Rev. Letters 23, 23 (1969).
[8]D. H. Youngblood, B. H. Wildenthal, and C. M. Class, Phys. Rev. 169, 859 (1968).
[9]R. Huby and J. R. Mines, Rev. Mod. Phys. 37, 406 (1965).
[10]F. S. Levin, Ann. Phys. (N.Y.) 46, 41 (1968).
[11]B. M. Bardin and M. E. Rickey, Rev. Sci. Instr. 35, 102 (1964).
[12]G. R. Satchler, Nucl. Phys. 55, 1 (1964).
[13]J. C. Hiebert, E. Newman, and R. H. Bassel, Phys. Rev. 154, 898 (1967).
[14]H. T. Fortune, T. J. Gray, W. Trost, and N. R. Fletcher, Phys. Rev. 179, 1033 (1969).
[15]P. D. Kunz, private communication.
[16]A. M. Lane and R. G. Thomas, Rev. Mod. Phys. 30, 257 (1958).
[17]J. B. French, in *Nuclear Spectroscopy*, edited by F. Ajzenberg-Selove (Academic Press Inc., New York, 1960), Part B, p. 890.
[18]W. J. Thompson, J. L. Adams, and D. Robson, Phys. Rev. 173, 975 (1968).
[19]B. W. Ridley, E. F. Gibson, J. J. Kraushaar, M. E. Rickey, and R. H. Bassel, Bull. Am. Phys. Soc. 11, 118 (1966).
[20]Received from F. G. Perey, Oak Ridge National Laboratory.
[21]W. F. Rich and C. E. Watson, to be published.
[22]J. P. Schiffer, Nucl. Phys. 46, 246 (1963).
[23]L. L. Lee, Jr., in *Proceedings of the International Conference on Nuclear Physics, Gatlinburg, Tennessee, 12-17 September 1966,* edited by R. L. Becker and A. Zucker (Academic Press Inc., New York, 1967), pp. 31–46.
[24]W. J. Gerace and A. M. Green, Nucl. Phys. A93, 110 (1967).
[25]P. Federman, G. Greek, and E. Osnes, Nucl. Phys. A135, 545 (1969).
[26]W. F. Rich, Ph. D. thesis, Rice University, 1967 (unpublished).

PHYSICAL REVIEW C VOLUME 2, NUMBER 2 AUGUST 1970

Proton Total Reaction Cross Sections in the 10–20-MeV Range: Calcium-40 and Carbon-12†

J. F. Dicello* and G. Igo‡
University of California, Los Alamos Scientific Laboratory, Los Alamos, New Mexico 27544
(Received 2 February 1970)

Total reaction cross sections for protons on ^{40}Ca have been measured at 15 energies between 10.3 and 21.6 MeV by the beam-attenuation method. The total reaction cross section for ^{40}Ca rises sharply at low energies, reaches a maximum value around 13 MeV, and reaches a minimum value around 16 MeV. The rise at the lower energies is a result of the Coulomb barrier. The dip at 16 MeV is probably associated with the (p,n) threshold for ^{40}Ca. A comparison is made between the present experimental values and preliminary optical-model predictions based on available elastic-scattering data and polarization data. The variation in the reaction cross section is also compared with the integrated partial cross sections for elastic scattering. Total reaction cross sections for protons on carbon have been measured at ten energies between 9.88 and 19.48 MeV. Resonances in the total reaction cross section are observed in the neighborhood of 10.4 and 13.8 MeV. Variations of 200 mb are seen in the cross sections with changes in energy of the incident protons of about 200 keV. A comparison is made of the present total reaction cross sections and the integrated partial cross sections for elastic scattering and inelastic scattering to the first excited state of ^{12}C.

I. INTRODUCTION

There exists a limited amount of data[1,2] regarding the variation of the total reaction cross section as a function of energy. Such data are necessary for determining optical-model parameters over a particular range of energies. Measurements for ^{40}Ca and ^{12}C of this kind are presented in this paper. The differential elastic cross sections for ^{40}Ca in the same energy region also have been measured.[3] Polarization data for ^{40}Ca in the same region have been obtained by Baugh *et al.*,[4] Rosen *et al.*,[5] and Bercaw and Boschitz.[6]

Considerable information regarding differential cross sections for carbon is available[7-15] in the region from 9 to 20 MeV. However, only a limited amount of data is available for proton total reaction cross sections, σ_R, in the same region. Makino, Waddell, and Eisberg[16] have examined the total reaction cross section of ^{12}C as a function of

energy above 16.5 MeV. These measurements indicate that σ_R varies relatively smoothly in this energy region. However, from 10 to 17 MeV, there are values only at 9.85,[17] 9.94,[18] 10.16,[18] and 16.5 MeV.[19]

These data are insufficient to determine the nature of the variation of σ_R as a function of energy. Differential cross-section measurements[10] for protons on ^{12}C show that the integrated partial cross sections for the first excited state of ^{12}C vary significantly as a function of energy between 9 and 16 MeV. Since the cross section for the first excited state of ^{12}C is large (150 to 400 mb) in this region, it is suggested that there could be considerable variation in σ_R.

There is considerable interest in the total reaction cross section of ^{12}C in connection with the response of plastic scintillators to protons in this energy range.

II. PROCEDURE

The beam-attenuation technique used in this work is similar to the method used previously.[20] It will be reviewed here briefly to point out the changes made for these measurements.

A. Experimental Method

The system used in the present experiment is illustrated in Fig. 1. A beam passes through two passing counters, 2 and 3, whose outputs activate a coincidence circuit. The output of the coincidence circuit is I_0, the total number of protons involved in the measurement of the reaction cross section. A significant number of protons are deflected from the collimated beam by elastic scattering, inelastic scattering, or multiple Coulomb scattering. These are removed from consideration by the use of anticoincident collimating counters, 1, 4A, and 4B, which also feed the I_0 coincidence circuit. The emergent beam of intensity I_0 is then incident on the target.

The unscattered beam passes through counter 5 and into a beam stopper. Scattered charged particles were detected in counter 6, a lithium-drifted silicon detector. The energy resolution obtained in counter 6 was ±200 keV. The major contribution to the width was due to the kinematical broadening associated with the large solid angle of acceptance. Counter 5 subtended a scattering angle of $\pm 12\frac{1}{2}°$. The corresponding solid angle is small, and the correction for inelastic events into counter 5 was smaller than the error due to a number of sources outlined below and was neglected. The expression for the total reaction cross section which is appropriate is

$$\sigma_R - \sigma_{CE} = \frac{I_0 - I}{nxI_0} - \frac{i_0 - i}{nxi_0} - \int_{\theta_C}^{\pi} \left(\frac{d\sigma}{d\Omega}\right)_{el} d\Omega , \qquad (1)$$

where σ_R is the total reaction cross section, σ_{CE} is the compound elastic cross section, I_0 and I are the beam incident on the target and the attenuated beam, respectively, with the target in, i_0 and i are the corresponding quantities with the target out, n is the atomic density of the target, x is the thickness of the target, θ_C is the angle subtended by counter 6, and $(d\sigma/d\Omega)_{el}$ is the differential elastic cross section. The quantities I_0, $I_0 - I$, i_0, $i_0 - i$, and nx are measured directly. The third term on the right is calculated from the available differential elastic-scattering data.

There is a small, but finite, "dead" layer on the front surface of a plastic scintillator used as a stopping counter. This is a region where an incident particle may go undetected because the energy lost in the plastic scintillator is insufficient to be detected when converted to light. There are two possible causes for this. Before the incident particle has lost sufficient energy by energy-loss mechanisms to be detectable, a nuclear interaction occurs which produces only uncharged decay products (neutrons) or charged decay products of insufficient energy to be detected. Alternatively, the incident particle may be scattered nearly 180° and out of the scintillator without losing sufficient energy in the scintillator.

It is necessary that the *change* in the cross sections for processes that contribute to the "dead" layer in counter 5 with the target in and out be negligible. To determine the magnitude of the change to be expected, the total reaction cross section for carbon, the principal nuclear constituent in plastic scintillator, was measured in approximately 300-keV steps over the region of interest.

B. Targets

Carbon-12. Two separate targets were used for the measurements of the total reaction cross section on carbon. Each target was self-supporting natural carbon of 99% purity. One target, having an areal density of 0.015 g/cm^2 (460 keV for 19.46-MeV protons), was used for measurements at 17.41 and 19.46 MeV. The other target, having an areal density of 0.00449 g/cm^2 (185-keV energy loss for 10-MeV protons), was used for all other measurements. The areal density was determined in the following manner. After the measurements were completed, the area of the target bombarded by protons, 0.100 in. in diameter, was punched out and weighed. The diameter of the punched portion of the target was measured with the use of a calibrated microscope. The targets were examined for roughness and irregularities, and

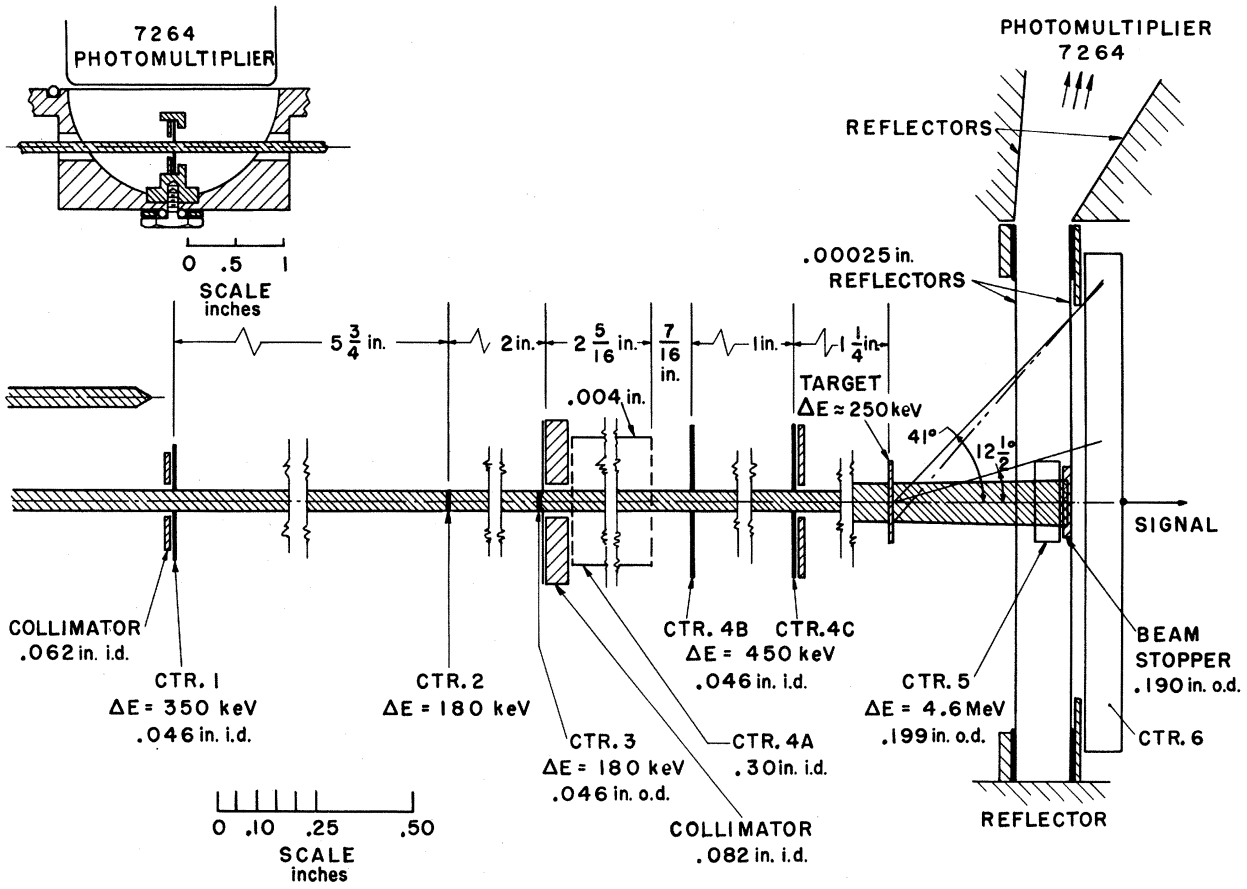

FIG. 1. A schematic diagram of the σ_R apparatus. The arrow at the left shows the shift in the position of the beam associated with a 250-keV shift in energy at 15.4 MeV. At the upper left, the configuration of a hemispherical reflector, collimator, and plastic scintillator are shown. Counter 4 consists of three sections, counter 4A, 4B, and 4C. Counter 4A is a tubular collimating counter $2\frac{5}{16}$ in. long. The indicated energy losses are for 15.4-MeV protons.

small corrections were made if necessary. The total uncertainty in the areal densities of the targets is ±4%.

With each target, a thin (0.002 47-g/cm^2) nickel foil was placed in front of the carbon. When a target-out run was made, a target holder with only a nickel foil mounted in it was placed in the normal position. The thin nickel foil was used in order to obtain an elastic profile for both target-out and target-in measurements (see Sec. II D-3).

Calcium-40. Four targets of ^{40}Ca were used for these total reaction measurements. It was desired to keep the targets as thin as possible so that structure in the reaction cross section as a function of energy could be observed. It was necessary to keep the targets sufficiently thick, however, so that the data could be obtained in a reasonable time. The thickness was chosen so that the average energy loss in the target was between 235 and 325 keV.

The targets were made from foils obtained from the Nuclear Division, Oak Ridge National Laboratory, Oak Ridge, Tenn. They contained 99.97% ^{40}Ca. The oxygen present in the foils was estimated to be less than 1% of the weight of the foils. Previous elastic-scattering measurements[3] carried out with targets made from the same foils confirm that the oxygen present in the foils was less than 1%. No other elemental impurity exceeded 0.08% of the weight of the foils, and the total percentage of elemental impurities was less than 0.13% of the weight of the foils. All operations with the target, including weighing and mounting, were performed in an argon atmosphere. Then the targets were placed in vacuum transfer chambers with which they could be placed in position in the σ_R apparatus and removed without exposure to air.

When the measurements of the cross sections had been completed the diameters of the targets were measured with a calibrated microscope. Each target was examined for irregularities and appropriate corrections were made. The areal densities of the four targets were 10.0, 10.3, 12.2,

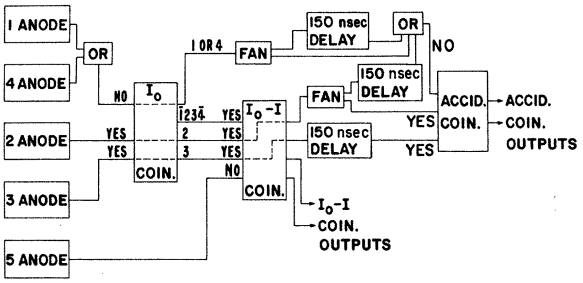

FIG. 2. A schematic diagram of the fast circuit. The outputs from the $I_0 - I$ coincidence circuit, and the outputs from the accidental coincidence circuit are used to trigger elements of the fast-slow circuit depicted in Fig. 3.

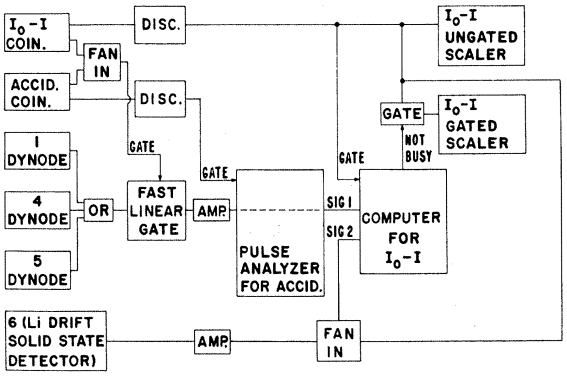

FIG. 3. A schematic diagram of the fast-slow circuit.

and 14.1 mg/cm^2. The uncertainty of the average areal density is ±2%. A more complete description of the method used for preparing and handling the targets is given in Ref. 3.

C. Electronics

The signals from the anodes of the photomultipliers were used to trigger elements of the fast circuit (see Fig. 2) in which the major part of the sorting of pulses was performed. After the initial selection of events, the $(I_0 - I)$ events defined as $(\bar{1}\ 2\ 3\ \bar{4}\ \bar{5})$ coincidences still contained a significant number of events in which one of the anticoincidence circuits had "failed." (The counters in coincidence are numbered as in Fig. 1; a bar means anticoincidence.) Some cases should occur in which a proton grazed one of the "no" counters, and the resulting anode pulse fell below the trigger level of the discriminator. Other cases could occur also in which the overshoot from a preceding pulse caused the anticoincidence requirement to fail. These erroneous events are removed by use of a fast-slow system (see Fig. 3) designed to examine the dynode outputs of all the anticoincidence counters for each of the $(I_0 - I)$ events. The $I_0 - I$ events are stored in a two-dimensional array. In one dimension, pulses from counter 6 were stored. Events having no pulse in counter 6 contribute to a peak at the low-energy end of the spectrum called the "miss peak."

The other dimension, called the OR direction, records pulses from counters 1, 4, and 5 which were not large enough to trigger the discriminator and to anti-out the $(I_0 - I)$ event. Those $(I_0 - I)$ pulses which are associated with 1-4-5 pulses should not be included in the final value of $I_0 - I$. The method for processing these data, in order to eliminate such events, will be discussed in Sec. II D.

Further, there are two classes of random pulses which had to be considered. The first of these was a noise pulse generated in passing counter 3 while, at the same time, a proton was scattered out by the beam by passing counter 2. A significant number of these random coincidences occurred. Such events depend strongly upon the noise noise from passing counter 3, and, although such events would cancel between target-in and target-out runs if the beam and noise levels were constant, in actual practice both beam and noise levels varied. Therefore, it was desirable that the number of these events be monitored during each run. This class of random coincidences was measured simultaneously with the real spectrum (see Fig. 2), and the results were displayed in a one-dimensional array (see Fig. 3).

It was also necessary to consider a noise pulse occurring in counter 5 which was large enough to trigger the discriminator. If the noise pulse occurred within the coincidence resolving time, a real $(I_0 - I)$ event was lost. These random coincidences were monitored with the circuitry shown in Fig. 4. An output from the I_0 coincidence circuit was fed into a "yes" input of a coincidence circuit. A pulse from the discriminator for the anode pulse from counter 5 was delayed 180 nsec

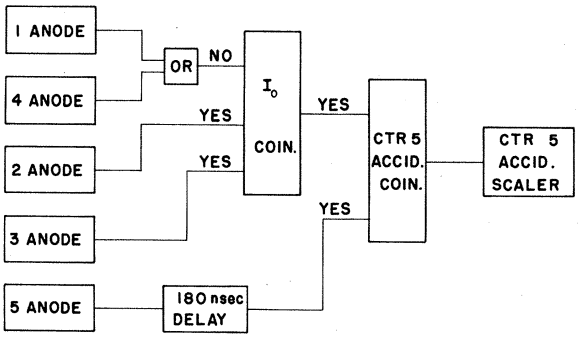

FIG. 4. A schematic diagram of the circuit used to measure random pulses in counter 5.

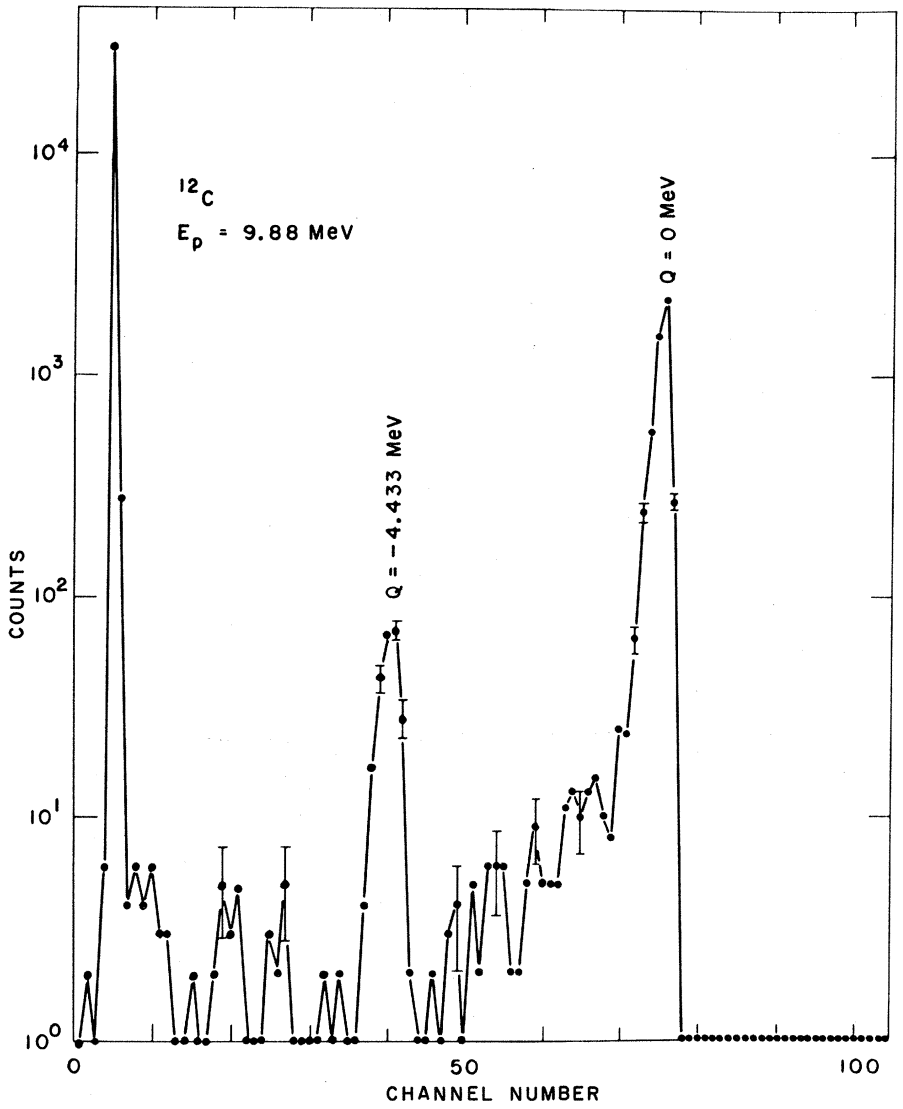

FIG. 5. Initial counter-6 profile. A typical spectrum is shown for ^{12}C summed in the OR direction and plotted in the counter-6 direction. The solid lines connect neighboring points. Typical errors are shown for some points.

and then fed into another "yes" input of the same coincidence unit. Only accidental coincidences between I_0 and counter 5 would produce an output pulse. In order to obtain the correct number of accidentals, the scaled output must be multiplied by $(I_0 - I)/I_0$. In practice, the noise level of counter 5 was always adjusted so that the number of these random events was negligible. Furthermore, the rate of random pulses in counter 5 was very nearly constant for both target in and target out, so that, to a good approximation, these events cancelled out.

D. Reduction of Data

The data from the ACCID analyzer (see Fig. 3) were read out on paper tapes and analyzed by hand. The data from the on-line computer, which recorded $(I_0 - I)$ information, were dumped onto magnetic tapes and were analyzed later with the help of an IBM 7094 computer.

The procedures followed in order to separate these data into the necessary components parts are outlined below.

1. *Separation of* OR *Events with Target In*

The data for a target-in run were first summed in the OR direction. Figure 5 shows a spectrum for ^{12}C with results plotted in the counter-6 direction. The miss peak appears in channel 5, the elastic peak in channel 76, and the first excited state of ^{12}C in channel 41. The spectrum contains some events in which one of the collimators was struck, but which were not eliminated by the $I_0 - I$ circuitry. It has been shown previously[20] that the elastic peak in the OR direction is free of events

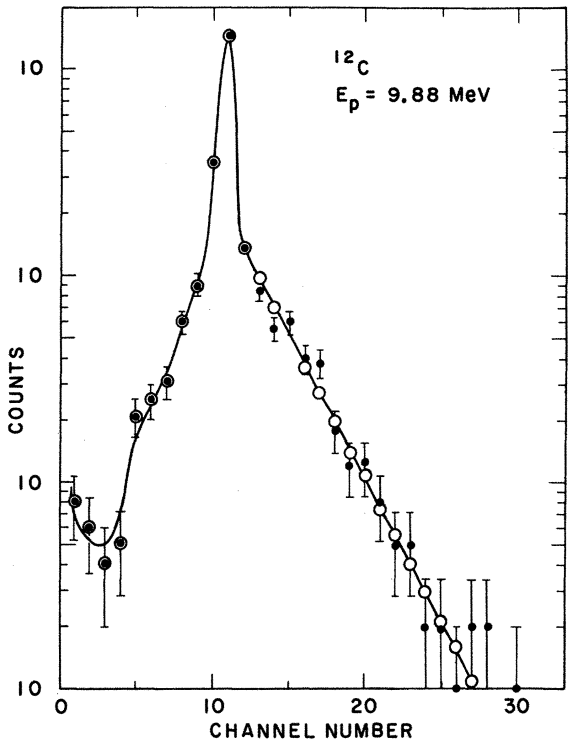

FIG. 6. The elastic profile and the elastic spectrum in the OR direction summed between channels 76 and 78 of counter 6 for ^{12}C. The closed circles are the elastic spectrum. The open circles are the elastic profile. The solid line is a visual aid only.

where the collimators or stopping counter have been struck, if the low-energy side of the elastic peak is excluded. Consequently, an upper and a lower channel in the counter-6 direction are chosen to bracket the elastic peak (e.g., channels 76 and 78 in Fig. 5). The computer sums in the counter-6 direction between the given channels, and displays the resulting spectrum in the OR direction (see Fig. 6). A profile is chosen and fed back into the computer. Figure 6 shows the profile chosen, as well as the data points.

This profile in the OR direction can now be used to reject from the miss peak those events where a pulse was present in counter 1, 4, or 5 but which failed to anti-out. The elastic profile is normalized to the sum of counts between two specified channels on the low-energy end of the spectrum, usually between channel 2 and the peak channel. The result is shown in Fig. 7. Events on the high side of the peak, which are associated with unwanted OR events, are subtracted. Having removed the events containing an interaction with one of the OR counters, the computer presents a new counter-6 spectrum as shown in Fig. 8.

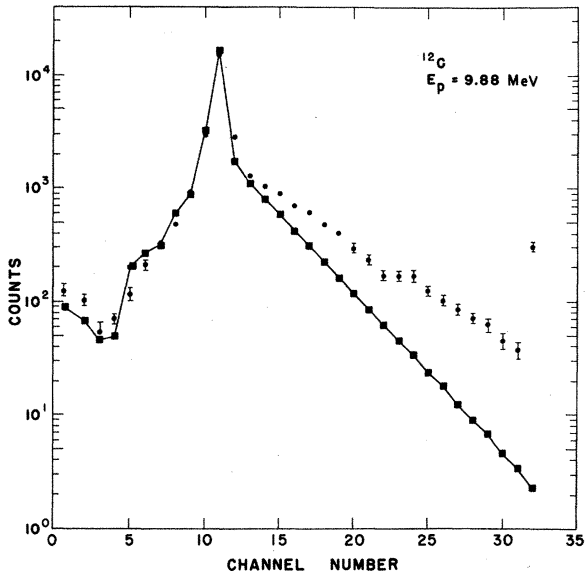

FIG. 7. The miss-peak spectrum in the OR direction for ^{12}C. The miss-peak spectrum versus OR channel, summed between channels 1 and 11 in the counter-6 direction, is denoted by the closed circles. The solid squares, which are connected by the solid line, are the normalized elastic profile.

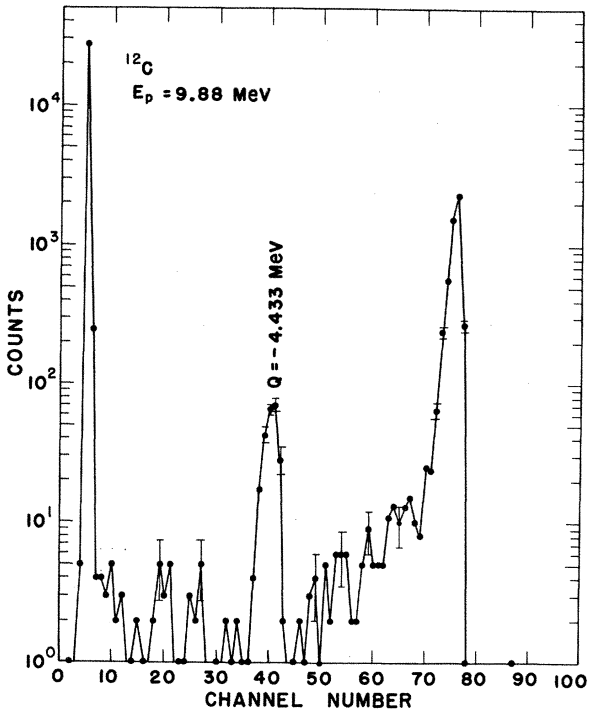

FIG. 8. Counter-6 spectrum, OR events removed from ^{12}C. The spectrum of counter 6 is summed over the OR channels with events eliminated where there was a pulse in counters 1, 4, or 5. Typical errors are shown for some points.

2. *Separation of Elastic Events for Runs with Target In*

The resolution of counter 6 was approximately 200 keV full width at half maximum for elastically scattered protons. The first excited state of ^{12}C has a Q value of -4.433 MeV. Therefore, the separation between the elastic peak and the first excited state is over 4 MeV, and eliminating the elastic peak was a simple matter. In some of the runs, the low-energy tail of the elastic peak intercepted the peak of the first excited state. However, the tail on the elastic peak is very close to an exponential tail. This, along with the fact that the region of overlap usually involved less than ten counts per channel, allowed the separation to be made quite simply. Note in Fig. 8 that there is some structure to the low-energy tail of the elastic peak. This is caused by the low-lying excited states of the nickel foil placed in peak. Dicello *et al.*[20] used the profiles from the target-in runs immediately before and after the target-out run. In the present measurements, thin (0.00247-g/cm^2) nickel foils were placed in the target holders for both target-in and target-out runs. This gave an elastic spectrum in the OR direction even for target-out runs (see Fig. 9). Since a nickel foil was present for both target-in and target-out runs, no correction had to be made for its presence. Therefore, the analyses of the target-out runs were identical to those previously described in this section for target-in runs.

3. *Elastic Correction*

Carbon-12. The elastic-scattering term in Eq. (1) was calculated using the data of Nagahara,[10] Daehnick and Sherr,[13] and Dickens, Haner, and Waddell.[12] The absolute errors in these data ranged between 2 and 7% with additional uncertainties on the relative values. The elastic correction ranged from 165 mb at 19.46 MeV to 456 mb at 10.72 MeV. An additional uncertainty of 100 mb in $\sigma_R - \sigma_{CE}$ in the vicinity of $E_p = 10.6$ MeV must be added to the absolute errors mentioned just above. Near $E_p = 10.6$ MeV, Nagahara[10] finds a sharp peak in the elastic cross section (see Fig. 10). The exact position of this peak is uncertain because of the absolute uncertainty in the energy scale (see Refs. 10 and 13 and the discussion which follows in this section). Therefore the elastic correction to $\sigma_R - \sigma_{CE}$ could be wrong *in the vicinity of* 10.6 MeV and thus contribute an additional error of 100 mb.

The elastic correction was calculated taking into account the finite size of the beam and the

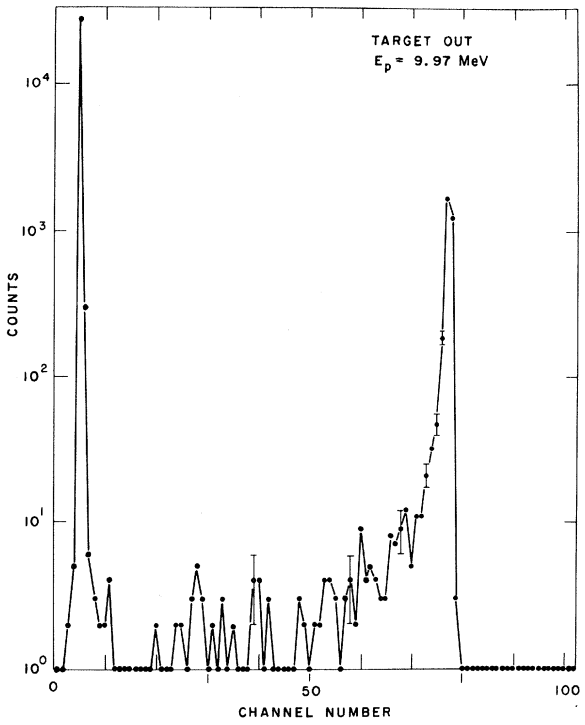

FIG. 9. A typical spectrum, with the target removed, summed in the OR direction for ^{12}C. The measurement was made with the nickel foil in the beam. Typical errors are shown for some points.

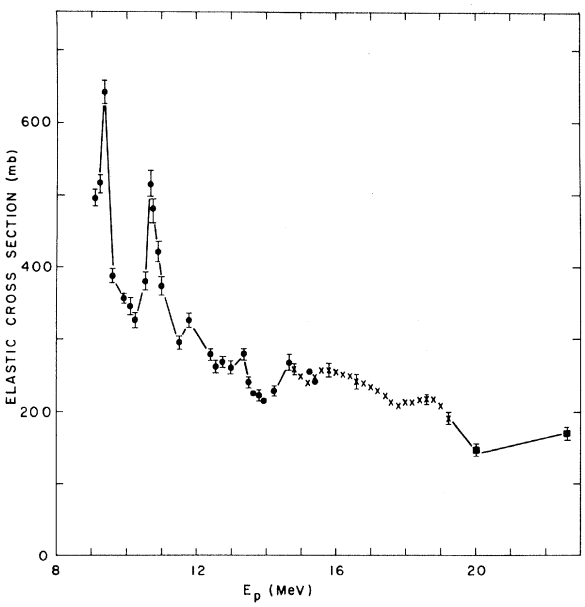

FIG. 10. The elastic correction for the total reaction cross section versus energy for ^{12}C. The solid circles were obtained from the data of Ref. 10, and the crosses are from the data of Ref. 13; the solid squares are from the data of Ref. 12. Typical errors are shown for some points.

TABLE I. Total reaction cross sections and quantities used in calculations for protons on carbon-12. All terms are defined in the text.

E_p (MeV)	nx (10^{20} cm^{-2})	I_0 (10^6)	$I_0 - I$	i_0 (10^6)	$i_0 - i$	$\int_{\theta_C}^{\pi} \left(\frac{d\sigma}{d\Omega}\right)_{el} d\Omega$ (mb)	$\sigma_R - \sigma_{CE}$ (mb)
9.88	2.25	25.266	27 632	25.459	24 695	354	195 ± 47
10.20	2.25	25.097	37 843	25.363	35 300	334	181 ± 53
10.40	2.25	25.187	38 374	25.449	34 155	371	434 ± 58
10.72	2.25	20.110	28 376	20.056	24 802	456	318 ± 61
13.51	2.25	25.846	21 411	25.833	18 848	231	207 ± 39
13.77	2.25	25.068	21 097	25.400	17 928	222	380 ± 43
14.54	2.25	26.569	21 593	26.423	17 971	264	324 ± 42
14.79	2.25	25.140	19 921	27.609	18 775	264	235 ± 40
17.41	9.79	25.166	24 857	24.345	10 829	212	343 ± 24
19.46	9.79	23.190	22 130	27.696	11 075	165	401 ± 24

angular distribution of multiple Coulomb scattering in the passing counters and in the target. The computer program used to make these calculations was developed by Roush.[21] The weighting function was obtained by following a distribution of trajectories through the counters and target, weighting each trajectory according to the distribution for multiple Coulomb scattering. The resulting elastic corrections are shown as a function of energy in Fig. 10. Since counter 6 subtends a half angle of 41°, these values are the weighted, integrated elastic cross sections from approximately 41° at 180° in the laboratory. The appropriate elastic corrections for each energy are listed in Table I.

The energies used for the data of Nagahara[10] in the present analyses are 300 keV higher than those listed by Nagahara. For example, the data said to be measured at 10.44 MeV by Nagahara are presented at 10.74 MeV. Daehnick and Sherr[13] observed that their data and Nagahara's data agreed better if there was a slight adjustment in the energy scale. If one compares both at 104.7° in the c.m. in the region around 14.5 MeV, one sees that a shift in energy of about 250 keV appears to give better agreement between the two excitation functions. It must be pointed out that the uncertainties in the absolute energy scale quoted in Refs. 10 and 13 do not exceed 150 keV when combined together. A shift in the absolute energy scale of the order of 200 keV can make a significant difference in the elastic correction for the total reaction cross sections. Therefore, higher-precision elastic-scattering measurements of carbon-12 would be most beneficial.

The energy scale for the elastic correction was determined in the following way. Nagahara's data show a sharp peak in the integrated elastic cross section around 10.4 MeV. The relative elastic cross sections measured by counter 6 for this present experiment were calculated as a function of energy. These represent the integrated elastic cross sections from approximately 13.5 to 44° in the c.m. system. The peak observed by Nagahara[10] at 10.4 MeV was observed in the present experiment at 10.7 MeV. Therefore, because of the improved agreement with the present data and with

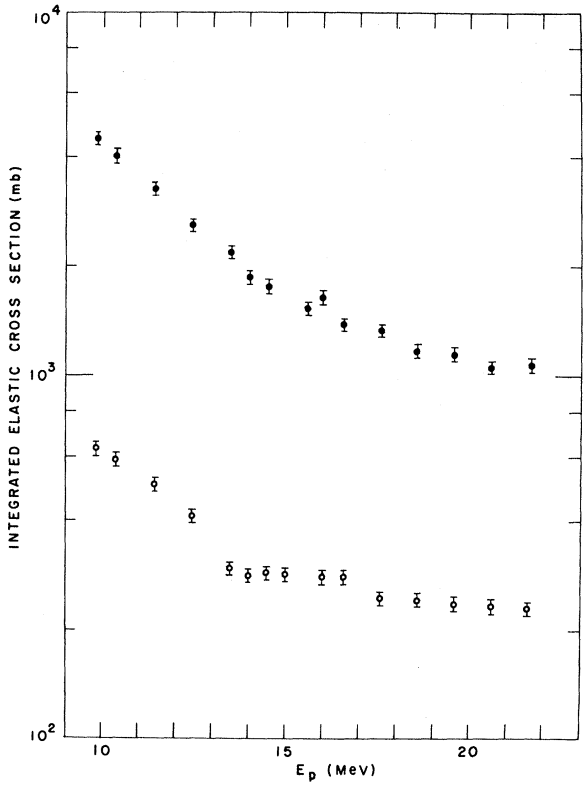

FIG. 11. Integrated differential elastic cross sections for ^{40}Ca. The open circles represent the elastic correction for the total reaction cross sections of ^{40}C. The closed circles are the integrated differential elastic cross sections of ^{40}Ca integrated from 12 to 180° in the lab system.

TABLE II. Total reaction cross sections for ^{40}Ca and quantities used in calculations. All terms are defined in the text.

E_p (MeV)	nx (10^{20} cm^{-2})	I_0 (10^6)	$I_0 - I$	i_0 (10^6)	$i_0 - i$	$\int_{\theta_C}^{\pi}\left(\frac{d\sigma}{d\Omega}\right)_{el} d\Omega$ (mb)	$\sigma_R - \sigma_{CE}$ (mb)
10.34	1.516	50.072	85 507	78.065	120 289	595	505 ± 59
11.38	1.516	50.837	53 695	50.350	43 647	508	736 ± 54
12.42	1.516	24.925	22 169	25.079	18 016	412	717 ± 63
12.42	1.516	25.108	25 828	25.085	21 415	412	742 ± 67
13.45	1.556	53.999	42 148	45.656	26 908	298	931 ± 46
13.46	1.516	50.634	53 003	54.210	46 465	298	953 ± 50
13.97	1.556	50.275	40 689	50.058	31 433	283	883 ± 44
14.48	1.556	57.375	44 556	50.050	30 045	287	846 ± 42
14.48	1.516	51.752	47 816	54.308	40 272	283	920 ± 47
14.97	1.843	50.709	23 410	25.196	6 491	285	822 ± 35
15.51	1.556	50.675	33 546	50.197	25 041	283	766 ± 39
16.49	2.125	50.821	39 601	50.854	28 342	279	765 ± 35
17.51	2.125	52.456	39 538	66.131	34 426	247	850 ± 34
18.54	2.125	50.023	35 450	42.614	20 568	243	821 ± 35
19.55	2.125	50.137	33 119	51.526	22 594	239	806 ± 33
20.57	2.125	50.744	32 372	48.283	19 665	235	851 ± 34
21.59	2.125	51.515	30 507	57.461	20 585	230	871 ± 32

the data of Daehnick and Sherr,[13] the data of Nagahara have been shifted 300 keV.

Calcium-40. The elastic corrections are plotted as a function of energy in Fig. 11, and the correction for each measurement is listed in Table II. The elastic corrections have an absolute uncertainty of ±4%.

III. TOTAL REACTION CROSS SECTIONS

Table I lists the total reaction cross sections for carbon-12, the proton energy E_p at the center of the target in the lab system, and the quantities that entered into the calculations of σ_R in Eq. (1). The uncertainty in the energy E_p is ±50 keV. The total reaction cross section versus energy is plotted in Fig. 12.

The total reaction cross sections for protons on ^{40}Ca between 10 and 22 MeV are shown in Fig. 13 and are listed in Table II. A value obtained by Turner *et al.*[22] at 28.5 MeV has been included in Fig. 13. Preliminary optical-model predictions by Perey[23] have been shown for comparison.

V. DISCUSSION

Carbon-12. We summarize the features of the total reaction cross sections for protons on carbon at ten energies between 9.8 and 19.5 MeV. An examination of the total reaction cross sections for carbon (see Fig. 12) shows that there is a sharp peak in the cross section at 10.4 MeV and

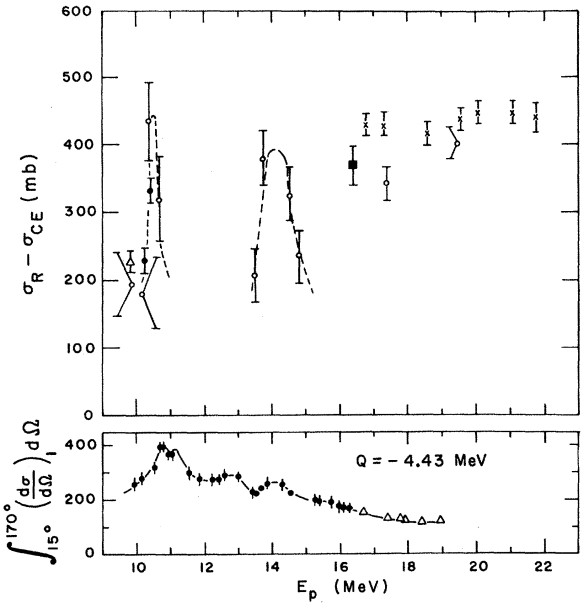

FIG. 12. The total reaction cross section versus energy for ^{12}C. The open circles are the results of the present experiment. The open triangle is from Meyer and Hintz (Ref. 17). The closed circles were obtained by Wilkins and Igo (Ref. 18); the closed squares, by Pollock and Schrank (Ref. 19); and the crosses, by Makino, Waddell, and Eisberg (Ref. 16). The bottom illustration consists of the integrated cross sections for the first excited state of ^{12}C ($Q = -4.433$ MeV) obtained by Nagahara (Ref. 10) using the differential cross sections from Ref. 10 (closed circles) and Ref. 7 (open triangles). The data of Ref. 10 have been shifted 300 keV (see Sec. II D–4).

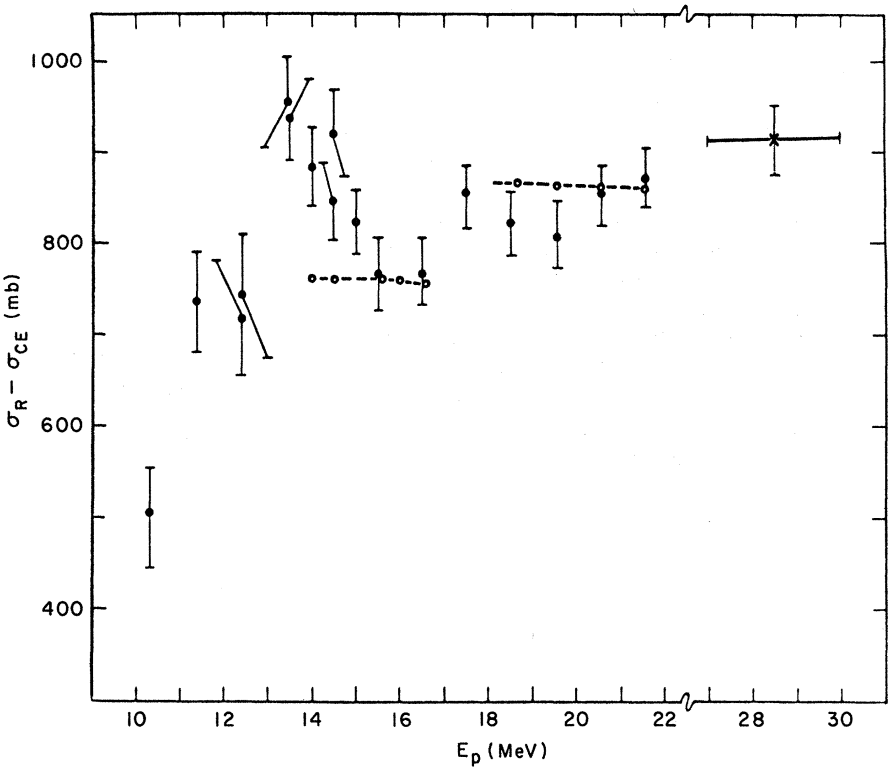

FIG. 13. Total reaction cross sections for protons on ^{40}C. The closed circles represent the data of the present experiment. The open circles are preliminary predictions by Perey (Refs. 23 and 28). The crosses are data obtained by Turner *et al.* (Ref. 22).

a broader peak centered at 14.0 MeV. Similar structures are seen in the integrated cross sections[10] for the first excited state of ^{12}C (see Fig. 12). The integrated elastic cross sections[10] for ^{12}C show minima in the same regions. A sharp level at 11.6 MeV in ^{13}N is well documented in the literature.[24] This level is reached at $E_p = 10.4$ MeV (lab) in the reaction of protons on carbon-12. A broad level (~500 keV) has been established earlier on the basis of the data of Nagahara[10] and Daehnick and Sherr[13] at 14.6 MeV.[24] The combined evidence obtained from the total reaction cross-section measurements for proton on carbon-12 in this paper, and in Refs. 10 and 13, suggest that this level may be approximately 200 keV higher. This broad level is reached in the reaction protons on carbon-12 at 14.0 MeV. According to the energy calibration obtained in the present work, the level is located at 14.85 MeV. Until more precise elastic-scattering data become available, the uncertainty in position will remain large. As would be expected in mirror nuclei, there are peaks in the n + carbon-12 reaction spectrum[25] which are the analogs of these peaks.[24] Figure 14 presents a comparison of the results of the measurements for elastic scattering into counter 6, obtained in the present total reaction cross-section measurements, and the elastic data of Refs. 10, 12, and 13.

In Sec. II A, it was stated that there exists a thin, but finite, "dead" layer in the stopping counter, counter 5. It was assumed that the effects of the layer were negligible in the present measurement. With the present results, a qualitative estimate of the change in the response of counter 5 as a function of energy can now be made.

Two causes of a change in the response of counter 5 were considered. The production of uncharged decay products is not of concern for the present experiment, since the threshold for neutron production on carbon is about 20 MeV in the lab system (carbon is the principal nuclear constituent in plastic scintillator). However, it is possible that the energy deposited in the counter may be insufficient to be detected. This may result either from charged decay products of insufficient energy to be detected, or because the incident particle may be scattered nearly 180° and out of the detector without depositing sufficient energy in the scintillator.

In Fig. 12, the data of the present experiment and the integrated cross sections for scattering to the first excited state of ^{12}C are presented. There are large changes in the total reaction cross section as a function of energy; however, most of the total reaction cross section at lower energies is a result of scattering to the first excited state of ^{12}C ($Q = -4.433$ MeV). The production of charged particles of very low energies is relatively small. This is in agreement with the previous results of

Measday.[26] Measday has shown that nuclear interaction in plastic scintillators consist primarily of excitations of low-lying states in this energy region. The dead layer in counter 5, then, must be primarily a result of back scattering from the front of counter 5 for the elastic and first excited states of ^{12}C.

A good estimate as to the magnitude of the change resulting from this dead layer can be made as follows. A conservative estimate of the loss of energy associated with the production of one photoelectron is 10 keV.[27] Counter 5 was set to trigger on noise, therefore the dead layer on counter 5 must be about 10 keV. In the region where there is the greatest change in the total reaction cross section with energy, namely around 10.4 MeV,

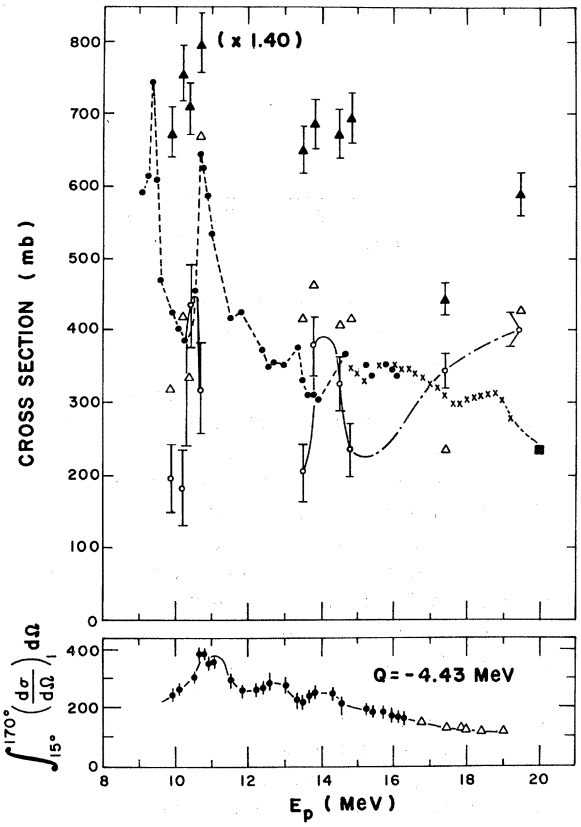

FIG. 14. Comparison of the total reaction cross section, the integrated elastic cross section, and the integrated inelastic cross section for the first excited state of ^{12}C. The lower illustration is the same as that in Fig. 12. In the upper illustration, the open circles indicate the total reaction cross section from the present experiment; the open triangles, the elastic scattering into counter 6 ($12\frac{1}{2}$ to 41° in the lab system) from the present experiment; the closed triangles, the elastic scattering into counter 6 plus the elastic correction from 41 to 180°; the closed circles, the crosses, and the closed squares indicate the integrated elastic cross section from 33 to 180° from Refs. 10, 12, and 13, respectively.

Wilkins[28] has integrated the differential cross sections for the elastic and first excited states from 65 to 180°. A change in energy of 300 keV corresponds to a change in this integrated cross section of about 150 mb. Since the targets used in the present experiment corresponded to an energy loss of about 300 keV, the correction to the present measurements is given approximately by

$$150 \text{ mb}\left(\frac{10 \text{ keV}}{300 \text{ keV}}\right) = 5 \text{ mb}. \tag{2}$$

This correction is small compared with the present experimental uncertainties and has been neglected.

Calcium-40. Preliminary optical-model analyses[23,29] of some of the differential elastic cross sections[3] and the polarization data[4-6] for ^{40}Ca have been completed. The experimental total reaction cross sections were not included in these initial analyses. Perey[23,29] analyzed the data in two groups. The data above 16.57 MeV were analyzed as one group, and the data from 13.98 to 16.57 MeV were

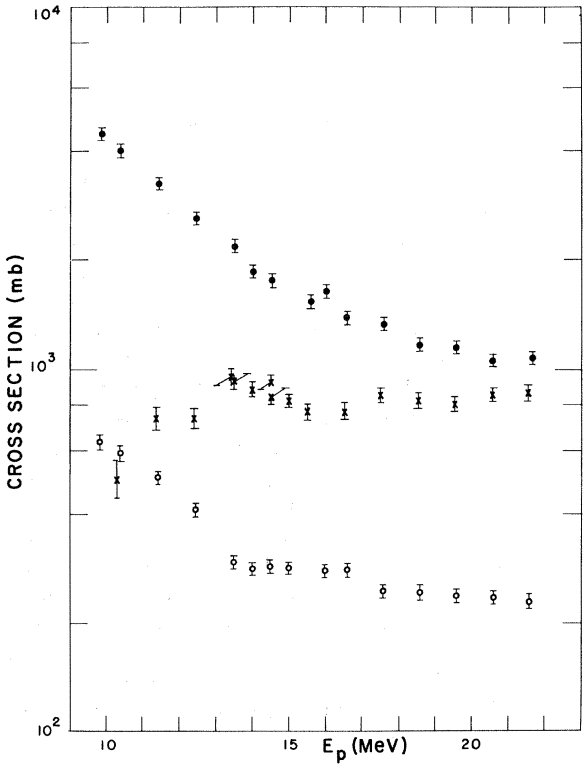

FIG. 15. Total reaction cross sections and the integrated elastic cross sections for ^{40}C. The crosses are the total reaction cross sections of the present experiment. The open circles are the elastic correction for the total reaction cross sections, integrated from 41 to 180° in the lab system. The closed circles are the integrated elastic cross sections, integrated from 12 to 180° in the lab system.

analyzed as a second group. [The (p,n) threshold for ^{40}Ca is approximately 16 MeV.] The fits to the differential elastic data and the polarization data are presented elsewhere. A comparison is made in Fig. 13 of the results of the optical-model analyses and the present results.

The total reaction cross section for ^{40}Ca rises sharply at low energies, reaches its maximum value around 13 MeV, and reaches a minimum around 16 MeV (see Fig. 13). This dip is probably associated with the (p,n) threshold at 16 MeV. The rise at the lower energies is a result of the Coulomb barrier. The predictions of the optical-model analysis discussed previously agree reasonably well with the data at the higher energies, even predicting the dip aroung 17 MeV. There are no predictions available at the lower energies.

There seems to be a correlation between the maxima and minima observed in the total reaction cross sections and the integrated elastic cross sections (see Fig. 15). However, the uncertainties in the cross sections make any conclusion speculative. Those energies where a maxima or minima are observed in the total reaction cross sections are the same as the energies where minima or maxima seem to occur in the differential cross sections at the backward angles (140°). The optical-model analyses also gave the poorest fits to the elastic data in these same regions.

In conclusion, the ^{40}Ca data do show a certain amount of structure. However, the changes in the total reaction cross section with energy for ^{40}Ca are sufficiently gradual so that the optical model can be used with moderate success. For better quantitative agreement, it may be necessary, nevertheless, to analyze the ^{40}Ca data above and below the (p,n) threshold separately.

ACKNOWLEDGMENTS

We are indebted to the Physics Division of Los Alamos Scientific Laboratory for its excellent support of this research. We are especially grateful to W. T. Leland who aided in many ways in the completion of this work and to the P-9 group for providing outstanding experimental facilities.

---

†Work supported by the U. S. Atomic Energy Commission.

*A.W.U.-A.E.C. Graduate Fellow. Currently at the Radiological Research Laboratories of Columbia University, New York, New York. Part of this work was done in partial fulfillment for the degree of Doctor of Philosophy at Texas A & M University.

‡Now at the University of California, Los Angeles, California.

[1]E. J. Burge, Nucl. Phys. 13, 511 (1959).

[2]K. Bearpark, W. R. Graham, and G. Jones, Nucl. Phys. 73, 206 (1965).

[3]J. F. Dicello, G. Igo, W. T. Leland, and F. G. Perey, to be published.

[4]D. J. Baugh, G. W. Greenless, J. S. Lilly, and S. Roman, Nucl. Phys. 65, 33 (1956).

[5]L. Rosen, J. G. Beery, A. S. Goldhaber, and E. H. Auerbach, Ann. Phys. (N.Y.) 34, 96 (1965).

[6]R. W. Bercaw and E. T. Boschitz, private communication.

[7]R. W. Peele, Phys. Rev. 105, 1311 (1957).

[8]G. W. Greenless, L. Gioietta Kuo, and M. Petravic, Proc. Roy. Soc. (London) A243, 206 (1957).

[9]W. M. Gibson, D. J. Prowse, and R. Rotblat, Proc. Roy. Soc. (London) A243, 237 (1957).

[10]Y. Nagahara, J. Phys. Soc. Japan 16, 133 (1961).

[11]G. G. Shute, D. Robson, V. R. McKenna, and A. T. Berztiss, Nucl. Phys. 37, 535 (1962).

[12]J. K. Dickens, D. A. Haner, and C. N. Waddell, Phys. Rev. 132, 2159 (1963).

[13]W. W. Daehnick and R. Sherr, Phys. Rev. 133, B934 (1964).

[14]J. B. Swint, A. C. L. Barnard, T. B. Clegg, and J. L. Weil, Nucl. Phys. 86 119 (1966).

[15]A. C. L. Barnard, J. B. Swint, and T. B. Clegg, Nucl. Phys. 86, 130 (1966).

[16]M. Q. Makino, C. N. Waddell, and R. M. Eisberg, Nucl. Phys. 68, 378 (1965).

[17]V. Meyer and N. M. Hintz, Phys. Rev. Letters 5, 207 (1960).

[18]B. D. Wilkins and G. Igo, Phys. Rev. 129, 2198 (1963).

[19]R. E. Pollock and G. Schrank, Phys. Rev. 140, B575 (1965).

[20]J. F. Dicello, G. J. Igo, and M. L. Roush, Phys. Rev. 157, 1001 (1967).

[21]M. L. Roush, private communication.

[22]J. F. Turner, B. W. Ridley, P. E. Cavanagh, G. A. Gard, and A. G. Hardacre, Nucl. Phys. 58, 509 (1964).

[23]F. G. Perey, private communication.

[24]F. Ajzenberg-Selove, "Energy Levels of Light Nuclei: $A=13$" (to be published).

[25]D. M. Drake, J. C. Hopkins, and H. Condé, private communication.

[26]D. F. Measday, Nucl. Instr. Methods 34, 353 (1965).

[27]G. Igo, L. F. Hansen, and T. J. Gooding, Phys. Rev. 131, 337 (1963).

[28]B. D. Wilkins, Ph.D. dissertation, University of California, 1963 (unpublished).

[29]J. F. Dicello, G. J. Igo, W. T. Leland, and F. G. Perey, Bull. Am. Phys. Soc. 12, 1184 (1967).